Method to detect gravitational waves from an ensemble of known pulsars

Xilong Fan, Yanbei Chen, and Christopher Messenger

Phys. Rev. D **94**, 084029 — Published 20 October 2016

DOI: 10.1103/PhysRevD.94.084029

Method to detect gravitational waves from an ensemble of known pulsars

Xilong Fan,[1,2] Yanbei Chen,[3] and Christopher Messenger[2]

[1] *Hubei University of Education, 430205, Wuhan, Hubei, China*
[2] *SUPA, School of Physics and Astronomy, University of Glasgow, Glasgow, G12 8QQ, United Kingdom*
[3] *Theoretical Astrophysics 350-17, California Institute of Technology, Pasadena, CA 91125, USA*

Combining information from weak sources, such as known pulsars, for gravitational wave detection, is an attractive approach to improve detection efficiency. We propose an optimal statistic for a general ensemble of signals and apply it to an ensemble of known pulsars. Our method combines $\mathcal{F}$-statistic values from individual pulsars using weights proportional to each pulsar's expected optimal signal-to-noise ratio to improve the detection efficiency. We also point out that to detect at least one pulsar within an ensemble, different thresholds should be designed for each source based on the expected signal strength. The performance of our proposed detection statistic is demonstrated using simulated sources, with the assumption that all pulsars' ellipticities belong to a common (yet unknown) distribution. Comparing with an equal-weight strategy and with individual source approaches, we show that the weighted-combination of all known pulsars, where weights are assigned based on the pulsars' known information, such as sky location, frequency and distance, as well as the detector sensitivity, always provides a more sensitive detection statistic.

I. INTRODUCTION

Pulsars are believed to be rapidly rotating neutron stars (NSs) that can emit continuous gravitational wave (GW) radiation if their mass distributions are asymmetric [1]. Observations from first-generation GW detectors have placed upper limits on the amplitude of these GWs from the known galactic millisecond pulsars. This in turn allows constraints to be placed on the ellipticities of these NSs [2]. With the advanced detector era having recently begun with Advanced LIGO [3] in operation and Advanced Virgo [4], and KAGRA [5] close behind, we will soon be able to make observations of these sources with significantly increased sensitivity.

For each pulsar with known sky location and assumed GW phasing (as inferred from arrival times of its radio pulses), time and frequency-domain matched-filtering approaches [6–10] are commonly applied. The former has been used within the LIGO-Virgo Collaboration for the known pulsar searches and applies a Bayesian marginalisation strategy to the unknown system parameters [6]. The latter, frequency domain approach, known as the $\mathcal{F}$-statistic [8] performs an analytical maximization of the likelihood over the unknown parameters of each pulsar and it is this method that we will make use of for the remainder of this paper.

Combining sources to improve detection probability is an attractive approach to weak signal detection (e.g. detecting NS ellipticity from analysis of the GW stochastic background [11] and detecting gravitational-wave memory using binary black hole mergers [12]). Since GW detectors currently study ∼200 known pulsars, the existing detection strategy for this relatively large ensemble can be viewed as trying to detect each one separately, and then waiting for the first detection to appear. This is certainly the most obvious strategy to take, but not obviously the most optimal. Cutler and Schutz (CS hereafter) [13] proposed an alternative: first sum the $\mathcal{F}$-statistic from each pulsar, and then use that sum as a new detection statistic. In this initial study, CS used an equal weight for all the pulsars to be combined. One issue with this approach is that including pulsars which are likely to emit relatively weak GWs will decrease the signal-to-noise ratio (SNR) of the combined statistic. As indicated in their paper, the SNR of the combined statistic will decrease if the detection ensemble includes weak sources where the squared SNR is less than half of the average squared SNR for all observed pulsars. Therefore, to more efficiently detect GWs from an ensemble of all known pulsars, it seems sensible to investigate the effects of giving non equal weights to the pulsars within the ensemble.

In this paper, we will generalize the idea proposed by CS, by considering the prior distribution of GW strengths from the pulsars within the ensemble. After a brief introduction to pulsar GW emission and the $\mathcal{F}$-statistic, we will apply the general theory of hypothesis testing, and obtain a Neyman-Pearson criterion for detecting GWs from an ensemble of pulsars. This leads to an optimal detection statistic, which in idealized situations (i.e., when our prior knowledge of the signal and our model for the noise are an accurate representation of reality) provide the highest detection probability with a given false-alarm probability. As we will show, this statistic can in some cases be approximated by linearly combining $\mathcal{F}$-statistic values from the ensemble of pulsars with appropriate weights.

We assume that the ellipticities of pulsars follow a common (yet unknown) intrinsic distribution and that the orientation of their rotation axes are isotropically distributed. We then draw on our knowledge of their sky location, distance from the earth, and their rotation frequency to construct prior distributions on the expected GW amplitudes from our known pulsars. Since the intrinsic ellipticity distribution remains unknown, we model it as a simple exponential distribution, but perform tests using both exponential and Gaussian distributions.

This paper is organized as follows. In Sec. II, we briefly review the form of GW emission from individual pulsars and the $\mathcal{F}$-statistic; in Sec. III, we introduce the optimal statistic for a general ensemble of pulsars and discuss how it may apply to a set of pulsars in idealized situations; in Sec. IV, we test our statistic on two possible intrinsic distributions of pulsar ellipticity. We summarize our main conclusions in Sec. VI.

II. BRIEF REVIEW OF GW FROM KNOWN PULSARS AND THE $\mathcal{F}$-STATISTIC

In this section, we give a brief overview of the signal model and maximum-likelihood detection statistic for a single pulsar.

A. Gravitational Waveform

For a single GW detector, the signal strain as a function of time, $h(t)$, from

$$h(t) = \frac{16\pi^2\epsilon I f^2}{d}\left[\alpha_+\tilde{F}_+(t) + \alpha_\times\tilde{F}_\times(t)\right]\cos[\Phi(t)+\Phi_0]\,, \tag{1}$$

with

$$\alpha_+ = \frac{1+\cos^2\iota}{2}\cos2\psi + \cos\iota\sin2\psi\,, \tag{2}$$

$$\alpha_\times = -\frac{1+\cos^2\iota}{2}\sin2\psi + \cos\iota\cos2\psi. \tag{3}$$

Here we have assume the pulsar, at distance d from the earth, to be an triaxial ellipsoid rotating at frequency f around one of its minor axes, which stays constant in orientation. In [8] this is the case when the angle between the total angular momentum vector of the star and the star's axis of symmetry is $\pi/2$.

The pulsar is nearly spherical, with a moment of inertial I around its rotation axes, ϵ is its ellipticity, given by

$$\epsilon = \frac{I_1 - I_2}{I} \tag{4}$$

with I_1 and I_2 the two moments of inertia around the two principal axes that are orthogonal to the rotation axis. The above four quantities (d, f, ϵ, I) define the strength of the source as received at the detector.

In addition, $\tilde{F}_{+,\times}(t)$ are the (time-dependent, due to earth rotation) antenna patterns of the detector toward a source at the sky location of the pulsar, while $\Phi(t)$ defines the GW phase evolution inferred from its radio (or x-ray) pulsations. — both are considered known. For the type of emission we are considering, GW radiation will be emitted at twice the rotation frequency, $2f$, with additional modulations due to the orbital motion of the pulsar and the motion of the detector due to the earth's rotation and orbit.

Finally, we have the polarization angle ψ , the inclination angle ι that describes the pulsar's orientation, and Φ_0 an additional unknown GW reference phase, all of which we consider as unknown.

In terms of notation, our ι and ψ are the same as used in [8], while $\tilde{F}_+(t)$ and $\tilde{F}_\times(t)$ are respectively equivalent to $a(t)$ and $b(t)$ of [8] where we have assumed that the angle between the two interferometer arms equals $\pi/2$.

B. The single-pulsar $\mathcal{F}$-statistic

Under the assumption that the measured strain is a combination of a GW signal and additive detector noise n, with a single-sided noise special density $S_h(f)$, the "near optimal" statistic is given by the so-called $\mathcal{F}$-statistic, derived by Jaranowski, Krolak and Schutz [8]. For point hypotheses with no uncertain model parameters the maximum likelihood approach of the $\mathcal{F}$-statistic is optimal in the Neyman-Pearson sense whereby the detection probability $P_{\rm DE}$ is maximised at fixed false-alarm probability $P_{\rm FA}$. However, even for individual pulsar detection the signal model does include additional unknown model parameters in which case the truly optimal approach is Bayesian and requires marginalisation over those parameters [14]. Our investigation makes use of the $\mathcal{F}$-statistic as our input data and hence by association also suffers from a lack of total optimality. However, as shown in [15] the reduction in sensitivity of the $\mathcal{F}$-statistic over the fully optimal approach is slight.

For an observation time $T_{\rm obs}$, the $\mathcal{F}$-statistic satisfies a χ^2 distribution with 4 degrees of freedom (4-D) and has a non-centrality parameter equal to the squared optimal SNR ρ^2, defined by

$$\rho^2 = \frac{256\pi^4\epsilon^2 I^2 f^4 \mathcal{K}}{d^2}\frac{T_{\rm obs}}{S_h(2f)} \tag{5}$$

(note that $2f$ is approximately the gravitational-wave frequency) with

$$\mathcal{K} = \sum_{p,q=+,\times}\alpha_p\alpha_q F_{pq}\,,$$
$$F_{pq} = \frac{1}{T_{\rm obs}}\int_0^{T_{\rm obs}}\tilde{F}_p(t)\tilde{F}_q(t)dt\,. \tag{6}$$

The unknown quantities defining the optimal SNR are the ellipticity ϵ and the geometrical factors contained within $\alpha_{+,\times}$ describing the GW polarisation and orientation of the pulsar. Note that $F_{++} \neq F_{\times\times}$ and that averaging over many sidereal days leads to $F_{+\times} \to 0$ and so such terms can be ignored.

For $\alpha_{+,\times}$ we shall assume that ι and ψ are distributed according to a random orientation of the pulsar's rotation axis. In this case, points with coordinates $(\alpha_+, \alpha_\times)$ are distributed on the 2-D plane axisymmetrically around the origin, with modulus

$$\zeta \equiv \alpha_+^2 + \alpha_\times^2 = \frac{1 + 6\cos^2\iota + \cos^4\iota}{4} \tag{7}$$

and $\cos\iota$ uniformly distributed between -1 and $+1$. We can write

$$\mathcal{K} = \zeta\left[F_{++}\cos^2(2\tilde{\psi}) + F_{\times\times}\sin^2(2\tilde{\psi})\right] \tag{8}$$

with $\tilde{\psi}$ related to ψ by an offset,

$$4\tilde{\psi} = 4\psi - \arctan\frac{4\cos\iota(1+\cos^2\iota)}{\sin^4\iota} \tag{9}$$

hence uniformly distributed between 0 and 2π. In this paper, we shall simply generate an ensemble of binaries using uniformly distributed $\cos\iota$ and uniformly distributed ψ. The average of $\mathcal{K}$ over this ensemble is given by

$$\langle\mathcal{K}\rangle = \frac{\langle\zeta\rangle}{2}(F_{++} + F_{\times\times}) = \frac{2}{5}(F_{++} + F_{\times\times}) \tag{10}$$

It was shown by CS that for the detection of a single pulsar in a network of M detectors, the $\mathcal{F}$-statistic still satisfy a 4-D χ^2 distribution with a non-centrality parameter $\rho_{\rm net}^2 = \sum_i^M \rho_i^2$, where ρ_i^2 is the optimal single detector SNR as defined in Eq. 5.

C. Scaling of detectability with observation time

In our idealized treatment with Gaussian noise, the significance of detection only depends on the non-centrality parameter ρ^2, which is proportional to the observation time $T_{\rm obs}$. For this reason, the $T_{\rm obs}$ required for a detection with a particular confidence level will be inversely proportional to $\mathcal{K}$ and ϵ^2, or

$$T_{\rm det} = \frac{S_h(2f)d^2}{256\pi^4\epsilon^2 I^2 f^4 \mathcal{K}}\rho_*^2 \tag{11}$$

with ρ_* a threshold (or a sensitivity level for ρ) determined by the desired false-alarm probability ($P_{\rm FA}$) and detection probability ($P_{\rm DE}$), as we shall discuss below.

Let us follow a frequentist approach of hypothesis testing. Suppose X is our detection statistic, which is either a 4-D χ^2 distribution or a 4-D non-central χ^2 distribution with non-centrality parameter ρ^2. Let us first impose a detection threshold $X_{\rm th}$ on X, so that $P[X > X_{\rm th}|\rho^2 = 0] = P_{\rm FA}$, which leads to

$$\left(1 + \frac{X_{\rm th}}{2}\right)e^{-\frac{X_{\rm th}}{2}} = P_{\rm FA}\,. \tag{12}$$

where the threshold $X_{\rm th}$ is determined implicitly from $P_{\rm FA}$. If X now has a non-zero ρ^2, its probability of overcoming the threshold becomes the detection probability, or

$$P_{\rm DE} = P[X > X_{\rm th}|\rho^2]\,. \tag{13}$$

The threshold ρ_*^2 is determined by requiring that when $\rho^2 \geq \rho_*^2$, Eq. (13) provides a significant $P_{\rm DE}$.

III. THE DETECTION STATISTIC OF MULTIPLE PULSARS

In this section we will extend the single pulsar analysis approach of Sec. II C to apply to the detection of GWs from an ensemble of pulsars.

A. General Theory

To formulate how we might detect a combination of n nearby sources, let us consider the general problem of distinguishing the distribution of n random variables, $(X_1, \ldots, X_n)$ — between two probability densities p_A and p_B. Suppose we will have a region $\mathcal{V}$, and we claim A if $(X_1, \ldots, X_n) \in \mathcal{V}$, and B otherwise. In the context of GW detection A is without signal, while B is detection. In this way, our false-alarm probability will be

$$P_{\rm FA} = \int_{\bar{\mathcal{V}}} p_A(x_1, \ldots, x_n)dx_1 \ldots dx_n, \tag{14}$$

where $\bar{\mathcal{V}}$ represents not being within the region $\mathcal{V}$, and our detection probability will be

$$P_{\rm DE} = \int_{\bar{\mathcal{V}}} p_B(x_1, \ldots, x_n)dx_1 \ldots dx_n. \tag{15}$$

We will then have to find the region $\mathcal{V}$ for which $P_{\rm DE}$ is maximized given $P_{\rm FA}$. It is possible to find that the boundary of $\mathcal{V}$ should be given by

$$\mu p_A(x_1, \ldots, x_n) = p_B(x_1, \ldots, x_n)\,. \tag{16}$$

This is an implicit formula: given different values of the Lagrange multiplier μ, we will arrive at regions that have particular pairs of $(P_{\rm FA}, P_{\rm DE})$. For each pair, the detection probability is the maximum possible value given $P_{\rm FA}$. Operationally, the boundaries of all these $\mathcal{V}$'s are given by surfaces specified by Eq. (16). In other words, for data $X_{1,\ldots,n}$, if we define the likelihood ratio

$$\mathcal{L} = \frac{p_B(X_1, \ldots, X_n)}{p_A(X_1, \ldots, X_n)} \tag{17}$$

as a detection statistic, and by imposing a threshold, we will obtain the best $P_{\rm DE}$ with given $P_{\rm FA}$.

If we have various versions of B parameterized by a set parameters $\boldsymbol{\theta}$, we can further average over these possibilities with their prior probability distributions $w(\boldsymbol{\theta})$, such that

$$P_{\rm DE} = \int d\boldsymbol{\theta} w(\boldsymbol{\theta}) \int_{\bar{\mathcal{V}}} p_B(x_1, \ldots, x_n; \boldsymbol{\theta})dx_1 \ldots dx_n. \tag{18}$$

This simply arrives at modified boundaries of $\mathcal{V}$ given by

$$\mu p_A(x_1, \ldots, x_n) = \int w(\boldsymbol{\theta}) p_B(x_1, \ldots, x_n; \boldsymbol{\theta})d\boldsymbol{\theta} \tag{19}$$

meaning that

$$\mathcal{L} = \frac{\int w(\boldsymbol{\theta}) p_B(X_1, \ldots, X_n; \boldsymbol{\theta}) d\boldsymbol{\theta}}{p_A(X_1, \ldots, X_n)}. \quad (20)$$

This is in fact the same as the marginal likelihood ratio (the Bayes factor in a Bayesian approach) for obtaining the data $X_{1,\ldots,n}$ — therefore we have simply established the optimality of the Neyman-Pearson approach in our case.

B. Multiple Pulsars

In the detection of multiple pulsars, let us consider A to be n independent 4-D χ^2 distributions, and B to be n independent 4-D non-central χ^2 distributions, with non-centrality parameter $\lambda_1, \ldots, \lambda_n$ (for simplicity, we use λ rather than the optimal SNR ρ^2). Recall that for a k-D non-central χ^2 distribution, we have

$$p_{(k,\lambda)}(x) = \frac{1}{2} e^{-(x+\lambda)/2} \left(\frac{x}{\lambda}\right)^{k/4-1/2} I_{k/2-1}(\sqrt{\lambda x}), \quad x > 0. \quad (21)$$

where I is the modified Bessel function of the first kind. We can then write

$$p_A(x_1, \ldots, x_n) = p_{(4,0)}(x_1) \cdots p_{(4,n)}(x_n) \quad (22)$$

and

$$p_B(x_1, \ldots, x_n) = p_{(4,\lambda_1)}(x_1) \cdots p_{(4,\lambda_n)}(x_n) \quad (23)$$

Following Eq. 16, for fixed values of $\lambda_1, \ldots \lambda_n$, we have

$$\prod_{j=1}^{n} \frac{2e^{-\lambda_j/2} I_1\left(\sqrt{\lambda_j x_j}\right)}{\sqrt{\lambda_j x_j}} = \mu \quad (24)$$

as optimal boundaries of $\mathcal{V}$ which can also be written as

$$\sum_j \log\left[\frac{I_1\left(\sqrt{\lambda_j x_j}\right)}{\sqrt{\lambda_j x_j}}\right] = \text{const}. \quad (25)$$

This shows how signals should be combined resulting in our combined detection statistic

$$\mathcal{L}^{\text{opt}}_{\text{fix}} = \sum_j \log\left[\frac{I_1\left(\sqrt{\lambda_j X_j}\right)}{\sqrt{\lambda_j X_j}}\right] \quad (26)$$

where $X_{1,\ldots,n}$ are the n observables.

If each λ depends on a set parameters $\boldsymbol{\theta}$, and for each j there is a corresponding prior distribution $w_j(\boldsymbol{\theta})$, then from Eq. (19), we can write

$$\mathcal{L}^{\text{opt}} = \sum_j \log\left[\int w_j(\boldsymbol{\theta}) e^{-\lambda(\boldsymbol{\theta})/2} \frac{I_1\left(\sqrt{\lambda(\boldsymbol{\theta}) X_j}\right)}{\sqrt{\lambda(\boldsymbol{\theta}) X_j}} d\boldsymbol{\theta}\right]. \quad (27)$$

As a sanity check, if $w_j(\lambda) = \delta(\lambda - \bar{\lambda}_j)$, we recover the previous result.

C. Special case: exponential distribution

We can further simplify the construction of the optimal statistic, simply and arbitrarily assuming that each λ_j value is drawn from an exponential distribution, or

$$w_j(\lambda) = \frac{1}{\bar{\lambda}_j} e^{-\lambda/\bar{\lambda}_j}, \quad \lambda > 0, \quad (28)$$

where $\bar{\lambda}$ is the mean value of the prior distribution on λ for each pulsar. In this case, we obtain the following closed-form expression,

$$\mathcal{L}^{\text{opt}}_{\text{exp}} = \sum_j \log\left[\frac{e^{Y_j} - 1}{Y_j}\right] \quad (29)$$

with

$$Y_j = \frac{\bar{\lambda}_j}{\bar{\lambda}_j + 2} \frac{X_j}{2} \quad (30)$$

This is quite interesting: those sources with $\bar{\lambda}_j \gg 2$ (already quite detectable individually), should be combined with a similar weight, while those much less than unity should be combined according to the expectation value of the non-centrality parameter, $\bar{\lambda}_j$. The latter case will be discussed further below.

D. Special Case: Weak-signal limit

A different way to obtain an optimal statistic is to directly assume that we should linearly combine the $\mathcal{F}$-statistic according to

$$\mathcal{L}^{\text{wopt}}_{\text{lin}} = \sum_j \alpha_j X_j, \quad (31)$$

and optimize the "signal-to-noise ratio", which is given by the increase of $\langle \mathcal{L}^{\text{wopt}}_{\text{lin}} \rangle$ due to non-zero λ_j divided by the variance of $\mathcal{L}^{\text{wopt}}_{\text{lin}}$ in the absence of signal. **This leads to**

$$\begin{aligned} \alpha_j &\propto \bar{\lambda}_j \\ &= \frac{f_j^4 \langle \mathcal{K}_j \rangle}{d_j^2 S_h(2f_j)}, \end{aligned} \quad (32)$$

where the second line is valid for known pulsars case, if we assume the intrinsic parameter of pulsars follows the same distribution (see discussion in Sec. V). This can be derive d from the optimal statistic, if we assume that we are interested in the low signal amplitude limit where the λ_j are small. In this case, we can Taylor-expand Eq. (27) and obtain, at leading order

$$\mathcal{L}^{\text{wopt}}_{\text{lin}} \approx \sum_j \frac{(X_j - 2)\bar{\lambda}_j}{4} \quad (33)$$

which is equivalent to using

$$\mathcal{L}_{\rm lin}^{\rm wopt} \approx \sum_j \alpha_j X_j, \tag{34}$$

which is also consistent Eq. (29) when $\bar{\lambda}_j$ is small.

This implies that if we could tolerate a high false-alarm probability by setting our threshold low, it is plausible that combining the observables proportional to the (prior) expectation value of non-centrality parameters would be optimal. However, as shown in Sec. IV, in the situations we encounter, this approximation is not quite valid.

E. Comparison With Individual Pulsar Detection

Before we compare our strategy with existing strategies that do not combine signals from multiple pulsars, let us first clarify what it means to "not combine signals". A careful examination provides two possible variants.

1. *Assigning equal false-alarm probability to each pulsar*

The first approach regards treating each pulsar as truly independent, and by setting the same false-alarm probability for each pulsar — even though each pulsar is not equally likely to provide detection. In this procedure, we therefore set the same threshold $X^{\rm th}$ for each pulsar, requiring

$$1 - P^n(X < X^{\rm th}|\rho^2 = 0) = P_{\rm FA} \tag{35}$$

and leading to the following total detection probability

$$P_{\rm DE} = 1 - \prod_{j=1}^{n} P(X < X^{\rm th}|\lambda_j) \tag{36}$$

of detecting at least one pulsar within this ensemble.

2. *Assigning false-alarm probability according to signal strength*

This is clearly problematic since we have potentially $\sim$ 200 pulsars — assigning the same false-alarm value to pulsars with dramatically different potential signal strength is clearly wasteful. If a different threshold is set for each pulsar, in such a way that the detection probability of a ensemble is maximum, we would then require

$$\begin{aligned}\mu &= \int w_j(\boldsymbol{\theta}) \frac{p_{(4,\lambda_j)}}{p_{(4,0)}} d\boldsymbol{\theta} \\ &= \int w_j(\boldsymbol{\theta}) \frac{e^{-\lambda(\boldsymbol{\theta})/2} I_1\left(\sqrt{\lambda(\boldsymbol{\theta}) X_j^{\rm th}}\right)}{\sqrt{\lambda(\boldsymbol{\theta}) X_j^{\rm th}}} d\boldsymbol{\theta}\end{aligned} \tag{37}$$

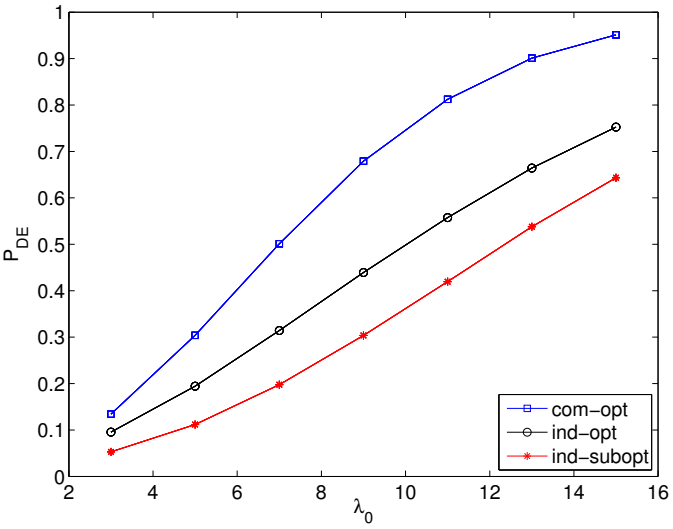

FIG. 1. (Color Online.) Detection probability for the model given by Eq. (39), using the optimal combined statistic (com-opt) and individual thresholds (ind-subopt for equal thresholds, see Sec. III E 1, and ind-opt for optimal thresholding, see Sec. III E 2). We have fixed $P_{\rm FA} = 0.01$.

where μ is a constant independent of j. As we vary μ, we obtain a varying set of $X_j^{\rm th}$ that would provide us with the optimal thresholds for each X_j, such that the total detection probability of detecting a GW signal within this ensemble is maximum given the false alarm probability (as defined in Eq. 35 with different $X^{\rm th}$).

IV. MONTE CARLO SIMULATIONS OF SIMPLE MODELS

In this section, we perform numerical investigations of two simple models. In particular, we will study the case of constant λ_j first, then the case where the λ_j values follow exponential distributions. This will provide important basic understanding before we move on to the known pulsars.

A. Constant λ_j

In this section, we shall perform Monte Carlo simulations for signals with fixed λ_j – the simplest case. We shall compare four strategies: (i) imposing a constant threshold on all X_j [Sec. III E 1], (ii) imposing a variable threshold on X_j, according to Eq. (37), **(iii) using a linear-combination statistic**

$$\mathcal{L}_{\rm lin} = \sum_{j=1}^{n} \alpha_j^{\beta} X_j \tag{38}$$

with various values of β, and (iv) the optimal statistic, according to Eq. (26).

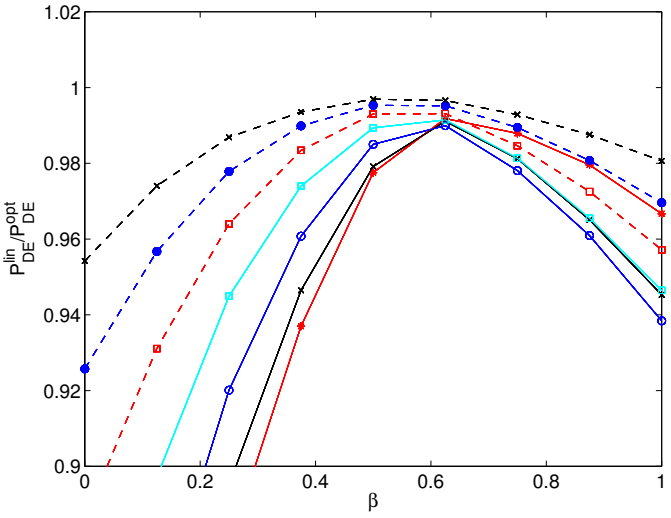

FIG. 2. (Color Online.) Detection probability of linear combination statistics [Eq. (38)] compared to the optimal detection probability. Different traces correspond to λ_0 ranging from 3 to 10, and we have fixed $P_{\rm FA} = 0.01$.

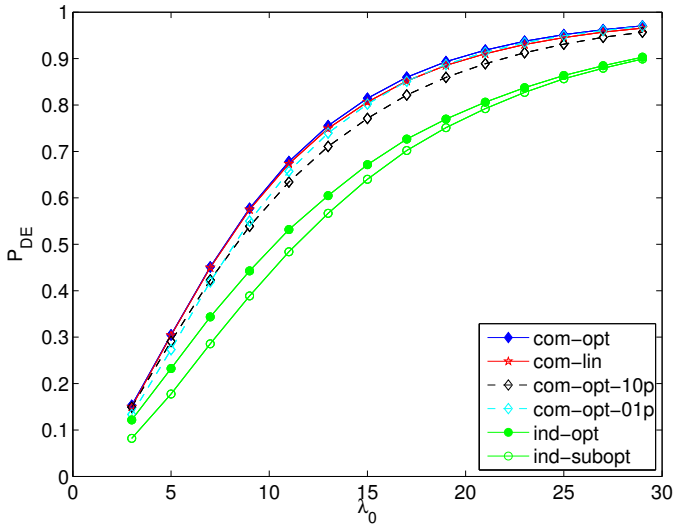

FIG. 3. (Color Online) Detection probability for models with λ_j following exponential distributions with mean value given by Eq. 39. We have fixed $P_{\rm FA} = 0.01$. Shown here are from the optimal statistic (com-opt), optimal statistic scaling prior distributions by 10 (com-opt-10p) and by 1/10 (com-opt-01p), linear combination statistic with $\beta = 1/2$ (com-lin), individual pulsar detection with optimal thresholding on each X_j (ind-opt) and individual pulsar detection with common threshold (ind-subopt).

We have chosen

$$\alpha_j = \lambda_j = \frac{\lambda_0}{j}, \quad j = 1, \ldots, 8, \tag{39}$$

which is designed to simulate an ensemble of sources that are distributed on a 2-D plane. If, within each disk with radius r, the number of sources will be proportional to r^2, then for the N-th source, its distance should be $\sim\sqrt{N}$, therefore non-centrality parameter should be $\sim 1/N$.

As we vary λ_0 from 3 to 15, and fixing $P_{\rm FA} = 0.01$, we compare the detection probability. As is shown by Fig. 1, the optimal strategy is substantially better than strategies (i) and (ii). In particular, in order for (i) and (ii) to achieve 50% detection probability, the non-centrality parameter must be a factor of ~ 2 stronger.

In Fig. 2, we investigate the performance of the linear-combination statistics. For $P_{\rm FA} = 0.01$, we plot $P_{\rm DE}$ as a function of the index β. It seems here that $\beta \sim 0.5$ performs slightly better than $\beta \sim 1$, although the optimal β value depends on λ_0, and is located somewhere between 0.5 and 0.8.

B. Exponential Distributions for λ_j

Let us now consider λ_j values that have simple exponential prior distributions for which we have analytical formulas derived in Sec. III C. This will also be important because we can test whether having the correct prior information in constructing the detection statistic can significantly affect detection efficiency. In particular, while the optimal statistic seems highly dependent on the prior distribution of λ, the linear statistic $\mathcal{L}_{\rm lin}$ is robust against a rescaling of the distributions of all λ_j.

Again, to be concrete, we chose now to have λ_j's follow exponential distributions, with mean values given by Eq. 39. The detection probability with $P_{\rm FA} = 0.01$ is shown in Fig. 3 for λ_0 ranging from 3 to 30. Here, we see again that the optimal statistic is substantially better than individually detecting the pulsars — while a more strategic thresholding allows some improvement.

In this case, we can see the potential benefits of the linear statistic: when the wrong prior distributions are used (with $\bar{\lambda}_j \to 10\bar{\lambda}_j$ and $\bar{\lambda}_j \to \bar{\lambda}_j/10$) to compute the optimal statistic, the detection efficiency drops to a level worse than using the linear statistic, which is independent of an overall rescaling of all λ_j values.

C. Scaling with the number of sources

Let us now consider how the detection probabilities of the various schemes scale with the number of sources. We do this by simply extending Eq. (39) to include a variable number of sources N.

In Fig. 4, we can see that as the number of sources increases the detection probability of the optimal and linear combination statistics with $\beta = 0.5$ also increases. The detection probability of individual pulsars using a common threshold decreases, while the individual detection with optimal thresholding also keeps increasing, but stops increasing at a relatively low number of sources. This can be explained as due to the combined statistics'

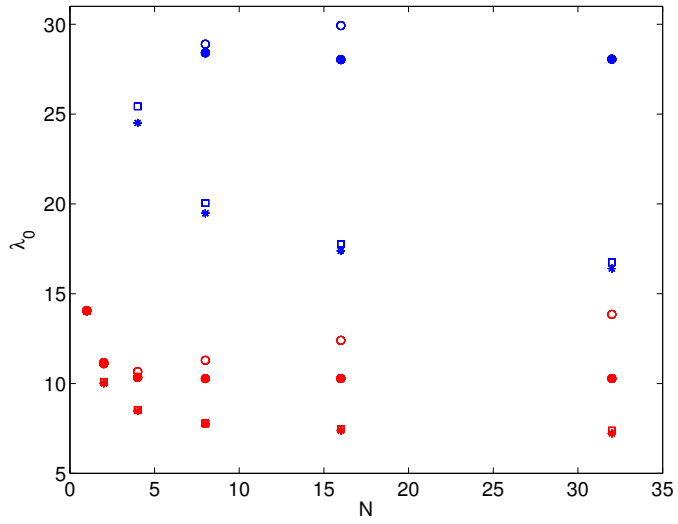

FIG. 4. (Color Online) Values of signal strength (λ_0) at which each detection strategy can yield detection probability of 50% (red symbols) and 90% (blue symbols), respectively, as function of the number of sources, N. We have used the optimal statistic (stars), linear combination statistic with $\beta = 0.5$ (square), uniform threshold for all sources (hollow circles) and optimal thresholding (solid circles). Increase of λ with N in the uniform threshold case indicates that including more sources will introduce contamination from weaker sources. We assumed exponential distributions for λ_j in this plot and have fixed $P_{\rm FA} = 0.01$.

ability to incorporate weaker sources without sacrificing sensitivity.

Numerically, we can see that a substantially larger signal strength has to be present for the individual detection strategies. In addition, we emphasize that the linear combination statistic, here shown to be very close to being optimal, is independent from an overall rescaling of the distribution of λ_j's. The optimal thresholding, on the other hand, does depend on the particular model of λ.

V. MONTE CARLO SIMULATIONS FOR KNOWN PULSARS

We shall now discuss the case of detecting GWs from multiple known pulsars. We will start by describing the known and unknown aspects of these sources, and then present the setup and conclusions of our numerical simulations.

A. Known Pulsars: prior distributions for λ_j.

For the case of multiple pulsars, the non-centrality parameter λ_j for each pulsar in a single detector is simply equal to ρ_j^2, as given by Eq. (5). We will now discuss in detail all factors contributing to our prior knowledge of ρ_j^2.

The ellipticity ϵ_j crucially defines the level of quadrupole deformation of the NS. At present, we have only theoretical constraints based on the internal structure of NSs, which span a wide range, and observational upper limits from from previous GW searches, which span the range $\sim 10^{-7} - 10^{-2}$ [2]. Our baseline assumption is that the ϵ of all pulsars follows a common (yet unknown) distribution; this could be motivated as arising from the belief that all these eccentricities were generated by the same physical mechanism. We note that it is plausible for Advanced LIGO to detect at the level of $\bar{\epsilon} \sim$ few $\times 10^{-8}$.

The geometrical factor $\mathcal{K}$ depends on the inclination angle ι, polarization angle $\tilde{\psi}$, and the antenna patterns F_{++} and $F_{\times\times}$, see Sec. II B. We shall assume no knowledge concerning the orientation of the pulsar, therefore uniformly distributing cosι between -1 and $+1$, and uniformly distributing $\tilde{\psi}$ between 0 and 2π. As for F_{++} and $F_{\times\times}$, they further depend on the geographical location and orientation of the detector, as well as the source's declination angle (the right ascension dependence is averaged away after many sidereal days observation).

As noted by CS, for the network of M detectors case, the non-centrality parameter of each pulsar is simply

$$\lambda_j^{\rm net} = \sum_i^M \lambda_{ji}^2, \tag{40}$$

B. Simulations and Results

Our simulations assume one year of observation using the network of Advanced LIGO and Virgo at design sensitivity [16] [17]. The positions and orientations of the detectors are taken from Table 1 of [8]. The known pulsar parameters (distance, sky location and frequency) used to compute $\lambda_j^{\rm net}$ are taken from the 195 known pulsars analysed in the initial detection era, and we assume that the moment of inertia $I = 10^{38}\,{\rm kg\,m^2}$ [10]. To provide a proof-of-principle of our proposed method, we assume (i) ϵ^2 values follow exponential distributions with two different rate parameters 4×10^{-16} and 9×10^{-16}, and (ii) ϵ values follow normal distributions with mean values of 1.5×10^{-8}, and 2×10^{-8} with standard deviations equal to half of their respective mean values.

We have performed simulations to test the detection efficiency of our proposed robust statistic $\mathcal{L}_{\rm lin}$ (Eq. 38, see discussion in IV) via the receiver operating characteristic (ROC) curve, which is a parametric plot of the probability of false alarm versus the probability of detection.

The ROC curve is constructed using 10^5 simulations of X_j with non-centrality parameter $\lambda_j^{\rm net}$ and 10^5 noise only simulations. With the assumption of ϵ^2 following the same distribution, **the $\alpha_j^{\rm net}$ is used in Eq. 38 to compute every simulated $\mathcal{L}_{\rm lin}$ in place of α_j for** M

detectors case, defined as

$$\alpha_j^{\rm net} = \sum_i^M \alpha_{ji} = \sum_i^M \frac{f_j^4 \langle \mathcal{K}_j \rangle}{d_j^2 S_{hi}(2f_j)}. \quad (41)$$

We compare the detection efficiencies of ensemble based strategies including the weighted-combination ($\beta = 0.5$) and equal-combination ($\beta = 0$, the CS case) method, with the individual pulsar detection strategy including the expected brightest (the largest value of $\frac{f^4\langle\mathcal{K}\rangle}{d^2 S_h(2f)}$), measured brightest (the maximum ρ_j^2 in each simulation) case.

The results are first presented in terms of answers to the following two questions: Will collecting more pulsars return higher $P_{\rm DE}$ values than an individual detection? How many sources should be combined to obtain the maximum $P_{\rm DE}$ at given $P_{\rm FA}$? As shown in Figs. 5 and 6 for various ellipticity distributions, the more sources combined, the higher is $P_{\rm DE}$ for our proposed robust statistic $\mathcal{L}_{\rm lin}$ with $\beta = 0.5$, although combining the weakest part of the population (e.g. the weakest 50 sources) will not greatly contribute to $P_{\rm DE}$. As expected, we find that the $P_{\rm DE}$ increases when combining the first few high amplitude sources, and then decreases for the equal weight method ($\beta = 0$) as more and more weak sources are added to the combination. These results are consistent with the simple test in Sec. IV. Since we do not know the true values of all pulsar parameters, it is interesting to ask whether the measured brightest source or the expected brightest source would be more detectable than any other ensemble of sources.

Since the weighted combination method is optimised for the whole population of GW signals, neither the measured brightest source nor the expected brightest one is more detectable than the whole population. This is not the case for the equal-weight combination method (see Fig. 5 and 6).

As shown in Fig. 7, our proposed weighted-combination method includes the known information of all sources and detectors, therefore combining all sources should yield a higher $P_{\rm DE}$ compared to other methods. In the case of $\overline{\epsilon^2} = 2 \times 10^{-16}$, given $P_{\rm FA} = 0.0001$, the $P_{\rm DE}{\sim}0.9$ for the weighted-combination method is a factor of $\sim$2 to 4 more sensitive than other methods (see top-left panel of Fig. 7). The improved performance of the weighted-combination method over other methods appears to be independent of the ellipticity distribution types and distribution parameter values used in our simulations.

The typical pulsar distance measurement error is $\sim$20% but could be up to a factor of 2-3 larger [e.g. 18]. To test the robustness of our proposed method, we test our sensitivity to distance uncertainty by drawing our pulsar distances from Gaussian distributions with mean values equal to the best estimated distance and with a standard deviation equal to 20% of the mean. As shown in Fig. 8, the distance uncertainties do not change the general performance of all methods: our proposed weighted-combination method still is the most efficient method and improves the $P_{\rm DE}$ by a factor of ~ 1.5 to 4 compared to different methods and given $P_{\rm FA} = 0.0001$. The level of improvement decreases when the GW signals become stronger.

VI. DISCUSSION

We have proposed a novel weighted-combination detection statistic for GWs from an ensemble of known pulsars. The aim of this approach is to improve the detection efficiency of GWs over that of individual pulsar detection based on the $\mathcal{F}$-statistic applied to single pulsars. The general argument behind the combination detection strategy is that a group of sources should be more detectable than an individual one if they share certain characteristics. We have shown that our general optimal statistic for the weighted combination of GW signals outperforms all other approaches.

We have shown that to more efficiently detect GW signals emitted from a ensemble of pulsars, each source within the ensemble could be assigned a different detection statistic threshold based on the expected signal strength. Furthermore, by assuming that the SNRs of all sources are constant or follow exponential distributions, we have shown that the linearly weighted-combination statistic is very close to being optimal and is robust to the choice of prior SNR distributions. These analytic and simple Monte Carlo tests predictions are consistent with results obtained from simulations of known pulsars.

We have also used the ROC function to determine the sensitivity of a range of possible search strategies where the detection probability between approaches is compared as a function of false alarm probability. To demonstrate the performance of the new weighted-combination detection method for the Advanced detectors era, we have compared the detection efficiency of the linearly weighted-combination method versus the equal-combination and individual detection method. We have done this by simulating GW signals emitted from the 195 known pulsars within the sensitive frequency band of Advanced LIGO and Virgo. We assume that the intrinsic pulsar parameter ellipticity ϵ^2 follows a common distribution in these simulations. The true form of the ellipticity distribution and its associated parameters are unknown. We have chosen to use both exponential and Gaussian distributions with mean values corresponding to ellipticities $\epsilon \sim 10^{-8}$, a value consistent with the initial GW era non-detection of pulsar signals and a possible advanced era detection. In general, the combination methods return better detection efficiency than a method that simply considers the closest or brightest pulsar. Being consistent with results of simple Monte Carlo tests, the most efficient method in simulations for known pulsars involves combining all known pulsars with weights $\propto \overline{\rho}$, the expected value of the optimal SNR of each pulsar. For the specific case where $\overline{\epsilon} \sim 1.5 \times 10^{-8}$, for one

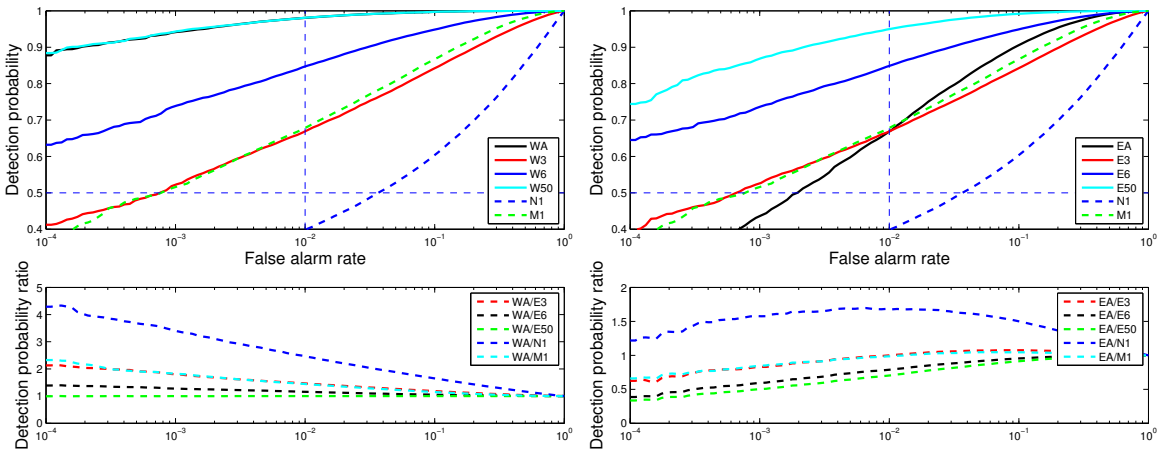

FIG. 5. ROC curves for different detection methods. WA (EA), W3 (E3), W6 (E6), W50 (E50), N1 and M1 correspond to weighted (equal) combinations of all, the expected brightest three, the expected brightest six, the expected brightest fifty, the expected brightest and the measured brightest pulsar(s) respectively. **The ϵ^2 in injections were drawn from** an exponential distribution with rate parameter 2×10^{-16}.

.

.pdf

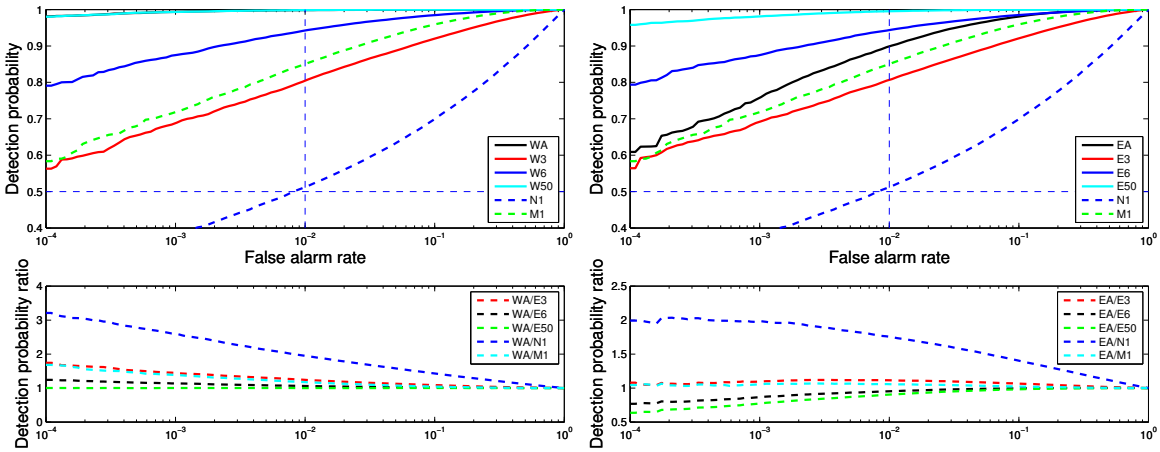

FIG. 6. Same as Fig. 5 but ϵ following the Gaussian distribution with mean value of 1.5×10^{-8}, and half of mean values as it variance value.

.

year observation of the Advanced detector network, we find that $P_{\rm DE}{\sim}0.95$ given $P_{\rm FA} = 0.0001$. In this case, the improvement by our proposed combined method could be up to a factor of ~ 4 compared with other methods. These results are consistent with the case of taking into account the measurement errors of pulsar distances.

An important feature of the proposed combination method is that it is very flexible. Using the new method it is simple to include more observed pulsars or updated source information (e.g. distance or orientation parameters) , without recalculating any individual detection $\mathcal{F}$-statistic values. However, we would expect that a fully Bayesian approach for combining all known pulsars may be more sensitive albeit at an increased computational cost.

The flagship known pulsar analysis within the GW community is a Bayesian approach [6, 7, 15, 19]. We note that it is likely that a comprehensive Bayesian approach to combining all known pulsars into a single analysis may produce a truly optimal result. Besides of all information discussed above, one could also consider the uncertainty of the major assumption (model) of this work: that all pulsars' ellipticity values follow a common but unknown distribution. **A hierarchical Bayesian approach would allow us to naturally investigate the true priors governing the distribution. In this**

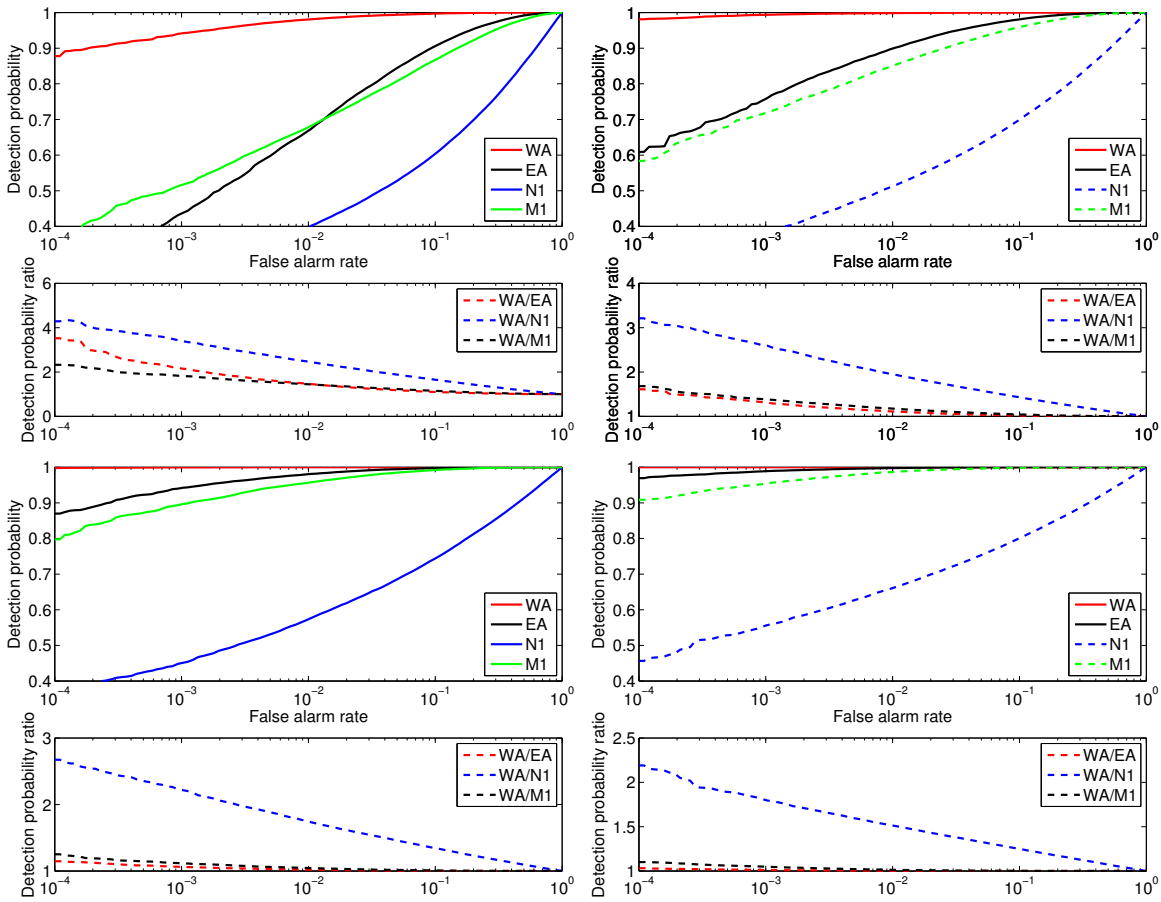

FIG. 7. ROC curves of the weighted-combination (WA), equal-combination (EA), the expected brightest (N1) and the the measured brightest (M1) detection methods for 10^5 signal injection simulations and 10^5 noise only simulations. WA and EA correspond to weighted and equal-combinations of all pulsars, respectively. **The intrinsic parameter in injections were drawn from** two distributions: (i) ϵ^2 follows an exponential distribution with rate parameter 2×10^{-16} (top-left panel) and 4×10^{-16} (bottom-left panel), and (ii) ϵ follows a Gaussian distribution with mean value of 1.5×10^{-8} (top-right) and 2×10^{-8} (bottom-right) with standard deviations equal to half of the mean value. Detection probability ratios (dashed lines) are shown in each panel.

.

case the form of the prior would be represented as a possible model and the parameters governing that distribution would be the "hype" parameters of that model. We could also apply Bayesian model selection to distinguish between different prior distributions e.g. exponential vs Gaussian or power law, etc... However, it is unclear how constraining such an analysis would be and we hope to tackle this problem in future studies. Beyond the detection of GWs emitted by a ensemble of pulsars, the posterior probability of all parameters could be output from a Bayesian approach. In future studies we hope to investigate such a Bayesian application to the detection of GWs from the ensemble of known pulsars.

ACKNOWLEDGMENTS

We would like to acknowledge valuable input from **our anonymous referee**, M. Pitkin and G. Woan, whose input has greatly improved the manuscript. XF acknowledges financial support from National Natural Science Foundation of China (grant No. 11303009 and 11673008). XF is a Newton Fellow supported by the Royal Society. YC is supported by NSF grants PHY-1404569 and C. M. is supported by a Glasgow University Lord Kelvin Adam Smith Fellowship and the Science and Technology Research Council (STFC) grant No. ST/ L000946/1.

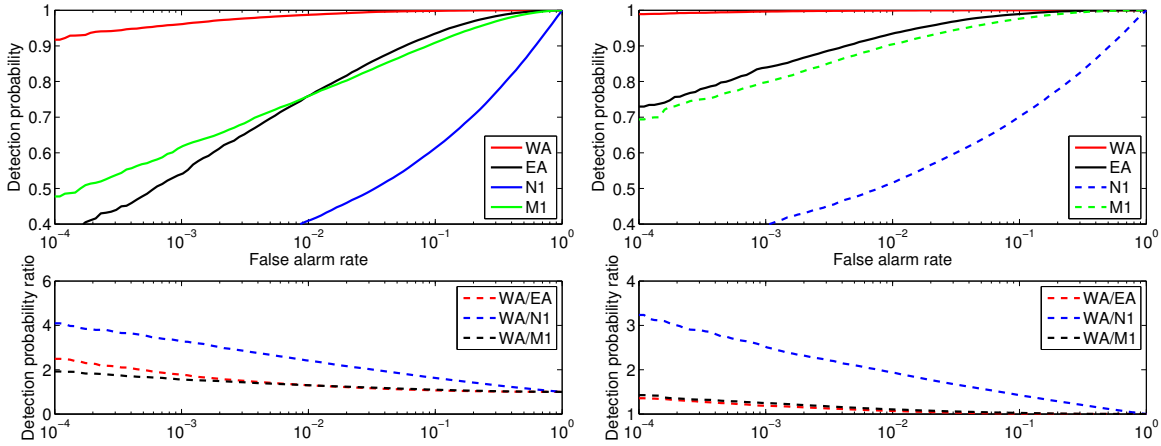

FIG. 8. The same as for the top panels of Fig. 7 but taking into account the measured distance error. The measured distance error effect is included by drawing "true" pulsar distances from a normal distribution with mean value equal to their current best estimates and a standard deviation of 20% of those mean values.

.

[1] M. Zimmermann and E. Szedenits, Jr., Phys. Rev. D **20**, 351 (1979).

[2] B. P. Abbott, R. Abbott, F. Acernese, R. Adhikari, P. Ajith, B. Allen, G. Allen, M. Alshourbagy, R. S. Amin, S. B. Anderson, and et al., Astrophys. J. **713**, 671 (2010), arXiv:0909.3583 [astro-ph.HE].

[3] LIGO Scientific Collaboration, J. Aasi, B. P. Abbott, R. Abbott, T. Abbott, M. R. Abernathy, K. Ackley, C. Adams, T. Adams, P. Addesso, and et al., Classical and Quantum Gravity **32**, 074001 (2015), arXiv:1411.4547 [gr-qc].

[4] F. Acernese, M. Agathos, K. Agatsuma, D. Aisa, N. Allemandou, A. Allocca, J. Amarni, P. Astone, G. Balestri, G. Ballardin, and et al., Classical and Quantum Gravity **32**, 024001 (2015), arXiv:1408.3978 [gr-qc].

[5] Y. Aso, Y. Michimura, K. Somiya, M. Ando, O. Miyakawa, T. Sekiguchi, D. Tatsumi, and H. Yamamoto, Phys. Rev. D **88**, 043007 (2013), arXiv:1306.6747 [gr-qc].

[6] R. J. Dupuis and G. Woan, Physical Review D **72**, 102002 (2005).

[7] M. Pitkin, Monthly Notices of the Royal Astronomical Society **415**, 1849 (2011), arXiv:1103.5867 [astro-ph.HE].

[8] P. Jaranowski, A. Królak, and B. F. Schutz, Phys. Rev. D **58**, 063001 (1998), gr-qc/9804014.

[9] J. Aasi, B. P. Abbott, R. Abbott, T. Abbott, M. R. Abernathy, T. Accadia, F. Acernese, K. Ackley, C. Adams, T. Adams, and et al., Classical and Quantum Gravity **31**, 165014 (2014), arXiv:1402.4974 [gr-qc].

[10] J. Aasi, J. Abadie, B. P. Abbott, R. Abbott, T. Abbott, M. R. Abernathy, T. Accadia, F. Acernese, C. Adams, T. Adams, and et al., Astrophys. J. **785**, 119 (2014), arXiv:1309.4027 [astro-ph.HE].

[11] D. Talukder, E. Thrane, S. Bose, and T. Regimbau, Phys. Rev. D **89**, 123008 (2014), arXiv:1404.4025 [gr-qc].

[12] P. D. Lasky, E. Thrane, Y. Levin, J. Blackman, and Y. Chen, ArXiv e-prints (2016), arXiv:1605.01415 [astro-ph.HE].

[13] C. Cutler and B. F. Schutz, Phys. Rev. D **72**, 063006 (2005), gr-qc/0504011.

[14] A. C. Searle, ArXiv e-prints (2008), arXiv:0804.1161 [gr-qc].

[15] R. Prix and B. Krishnan, Classical and Quantum Gravity **26**, 204013 (2009), arXiv:0907.2569 [gr-qc].

[16] LIGO Document T1200307-v4.

[17] LIGO Document T1300121-v1.

[18] J. H. Taylor and J. M. Cordes, Astrophys. J. **411**, 674 (1993).

[19] J. T. Whelan, R. Prix, C. J. Cutler, and J. L. Willis, Classical and Quantum Gravity **31**, 065002 (2014), arXiv:1311.0065 [gr-qc].